An Effector-Targeted Protease Contributes to Defense against *Phytophthora infestans* and Is under Diversifying Selection in Natural Hosts[1][W]

Farnusch Kaschani[2], Mohammed Shabab[2,3], Tolga Bozkurt, Takayuki Shindo, Sebastian Schornack, Christian Gu, Muhammad Ilyas, Joe Win, Sophien Kamoun, and Renier A.L. van der Hoorn*

Plant Chemetics Laboratory, Chemical Genomics Centre of the Max Planck Society, Max Planck Institute for Plant Breeding Research, 50829 Cologne, Germany (F.K., M.S., T.S., C.G., M.I., R.A.L.v.d.H.); and The Sainsbury Laboratory, John Innes Centre, Norwich NR4 7UH, United Kingdom (T.B., S.S., J.W., S.K.)

Since the leaf apoplast is a primary habitat for many plant pathogens, apoplastic proteins are potent, ancient targets for apoplastic effectors secreted by plant pathogens. So far, however, only a few apoplastic effector targets have been identified and characterized. Here, we discovered that the papain-like cysteine protease C14 is a new common target of EPIC1 and EPIC2B, two apoplastic, cystatin-like proteins secreted by the potato (*Solanum tuberosum*) late blight pathogen *Phytophthora infestans*. C14 is a secreted protease of tomato (*Solanum lycopersicum*) and potato typified by a carboxyl-terminal granulin domain. The EPIC-C14 interaction occurs at a wide pH range and is stronger than the previously described interactions of EPICs with tomato defense proteases PIP1 and RCR3. The selectivity of the EPICs is also different when compared with the AVR2 effector of the fungal tomato pathogen *Cladosporium fulvum*, which targets PIP1 and RCR3, and only at apoplastic pH. Importantly, silencing of *C14* increased susceptibility to *P. infestans*, demonstrating that this protease plays a role in pathogen defense. Although C14 is under conservative selection in tomato, it is under diversifying selection in wild potato species (*Solanum demissum*, *Solanum verrucosum*, and *Solanum stoliniferum*) that are the natural hosts of *P. infestans*. These data reveal a novel effector target in the apoplast that contributes to immunity and is under diversifying selection, but only in the natural host of the pathogen.

The defense response of solanaceous plants such as tomato (*Solanum lycopersicum*) is universal and includes the accumulation of proteins that are potentially harmful for pathogens, such as β-1,3-glucanases, chitinases, subtilases (e.g. P69B), and Cys proteases (e.g. PIP1 and RCR3; Tian et al., 2005, 2007; van Loon et al., 2006; Ferreira et al., 2007). These defense-related enzymes are thought to directly target the pathogens, for example by degrading their cell wall components. Successful tomato pathogens evolved means to suppress these defense responses. The oomycete late blight pathogen *Phytophthora infestans*, for example, secretes glucanase and subtilase inhibitors (Rose et al., 2002; Tian et al., 2004, 2005; Damasceno et al., 2008). In addition, the tomato-adapted fungal pathogen *Cladosporium fulvum* secretes chitin-binding AVR4 protein to protect its cell wall from host chitinases (van den Burg et al., 2006; van Esse et al., 2007).

Both *P. infestans* and *C. fulvum* also secrete inhibitors of papain-like Cys proteases (PLCPs) during infection. *C. fulvum* secretes AVR2, which mainly inhibits the tomato-secreted PLCPs PIP1 and RCR3 (Rooney et al., 2005; Shabab et al., 2008; van Esse et al., 2008). *P. infestans* secretes cystatin-like EPIC1 and EPIC2B proteins. EPIC1 inhibits RCR3, whereas EPIC2B inhibits both RCR3 and PIP1 (Tian et al., 2007; Song et al., 2009). These observations are consistent with the hypothesis that secreted enzymes that are potentially harmful for the pathogen are inhibited by pathogen-derived effectors.

An emerging concept in antagonistic host-pathogen interactions is that effector targets are under diversifying selection to evade manipulation (Hogenhout et al., 2009). Chitinases and glucanases, for example, are under strong diversifying selection (Bishop et al., 2000, 2005), possibly imposed by pathogen-derived inhibitors. In addition, the glucanase inhibitor GIP1 from *P. infestans* is also under diversifying selection, pointing to a potential molecular arms race between enzyme and inhibitor (Damasceno et al., 2008). Diversifying selection was also found in RCR3 and PIP1 in wild tomato species (*Solanum peruvianum*; Shabab

[1] This work was supported by the Max Planck Society, the Gatsby Foundation, the Deutsche Forschungsgemeinschaft (project nos. HO 3983/3–3 and HO 3983/7–1), the International Max Planck Research School, and the Council of Scientific and Industrial Research, New Delhi, India (Senior Research Fellowship to M.S.).

[2] These authors contributed equally to the article.

[3] Present address: Department of Bioorganic Chemistry, Max Planck Institute for Chemical Ecology, D–07745 Jena, Germany.

* Corresponding author; e-mail hoorn@mpipz.mpg.de.

The authors responsible for distribution of materials integral to the findings presented in this article in accordance with the policy described in the Instructions for Authors (www.plantphysiol.org) are: Renier A.L. van der Hoorn (hoorn@mpipz.mpg.de) and Sophien Kamoun (sophien.kamoun@bbsrc.ac.uk).

[W] The online version of this article contains Web-only data.

www.plantphysiol.org/cgi/doi/10.1104/pp.110.158030

et al., 2008). One of the variant residues in RCR3 was shown to prevent inhibition by AVR2 (Shabab et al., 2008). Other examples of antagonistic enzyme-inhibitor interactions at the plant-pathogen interface consistently show that positions at the enzyme-inhibitor interface are under selection pressure (for review, see Misas-Villamil and van der Hoorn, 2008).

Despite an abundance of biochemical and evolutionary data that support a role for effector-targeted proteases in pathogen defense, genetic support for the defense function of these enzymes is scarce. RCR3 contributes to resistance to *C. fulvum* and *P. infestans* (Dixon et al., 2000; Song et al., 2009). Furthermore, constitutive expression of the protease inhibitor AVR2 in transgenic Arabidopsis (*Arabidopsis thaliana*) and tomato results in plants that are more susceptible to a broad range of pathogens (van Esse et al., 2008).

So far, only the interactions of the *P. infestans* EPIC inhibitors with the host proteases PIP1 and RCR3 have been investigated (Tian et al., 2007; Song et al., 2009). Tomato, however, secretes seven PLCPs (Shabab et al., 2008). In this study, we investigated whether host proteases in addition to PIP1 and RCR3 can be inhibited by *P. infestans* EPICs. We discovered that tomato C14 is an additional target of the EPICs. We investigated the role of C14 in immunity using gene silencing and examined the natural variation of this protease in tomato and potato (*Solanum tuberosum*). These data demonstrate a role of C14 in *P. infestans* immunity and support the hypothesis that pathogens impose selection on their targets, but only in natural host species that have coevolved with the pathogen.

RESULTS

EPICs and AVR2 Target Different Host Proteases

To investigate the extent to which other secreted PLCPs of tomato are inhibited by EPICs, we produced each of the PLCPs by agroinfiltration and used extracts of agroinfiltrated leaves for activity-based protein profiling (ABPP) in the absence and presence of inhibitors. ABPP of PLCPs is based on the use of DCG-04, which is a biotinylated derivative of the PLCP inhibitor E-64 that irreversibly reacts with the active site Cys residue in a mechanism-dependent manner (Greenbaum et al., 2000). This technique was used to show that AVR2 inhibits RCR3 and PIP1 (Rooney et al., 2005; Shabab et al., 2008; van Esse et al., 2008), EPIC1 inhibits RCR3 (Song et al., 2009), and EPIC2B inhibits PIP1 and RCR3 (Tian et al., 2007; Song et al., 2009). The advantage of using ABPP is that proteases can be produced in planta and tested without purification, allowing us to test for selectivity in the presence of other proteases. Overexpression of the proteases by agroinfiltration results in strong additional signals upon DCG-04 labeling when compared with the signals of endogenous proteases (Supplemental Fig. S1).

To test which of the six tomato proteases are inhibited by AVR2, EPIC1, and EPIC2B, extracts containing the proteases were preincubated with these inhibitors and then incubated with DCG-04 to label the noninhibited proteases. In contrast to previous work with EPICs (Tian et al., 2007; Song et al., 2009), we chose conditions to select for strong interacting inhibitors by using long labeling times (5 h) at high DCG-04 concentration (2 μM) and low inhibitor concentration (66 nM). Under these conditions, weak, reversible interactions will not be detected, since DCG-04 reacts irreversibly and would eventually label all proteases. Preincubation of the protease-containing extracts with the inhibitors, followed by labeling with DCG-04, revealed that EPIC1 and EPIC2B prevent DCG-04 labeling of only C14, whereas preincubation with AVR2 prevents the biotinylation of only RCR3 and PIP1 (Fig. 1A). This remarkable selectivity indicates that, under stringent conditions, these inhibitors target different host proteases, forming tight complexes that persist over long incubation times.

To further test the strength of the EPIC-C14 interactions, inhibition assays were performed at lower EPIC concentrations and at different pH values. This showed that EPIC1 and EPIC2B inhibit C14 at nanomolar concentrations, indicating that EPIC1 and EPIC2B have a similarly strong affinity for C14 (Fig. 1B). In contrast, inhibition of PIP1 by AVR2 requires 10-fold higher AVR2 concentrations (Fig. 1B).

The pH of the apoplast is acidic (pH 5–6). Both C14 and PIP1 can be labeled from pH 4 to 7, indicating that

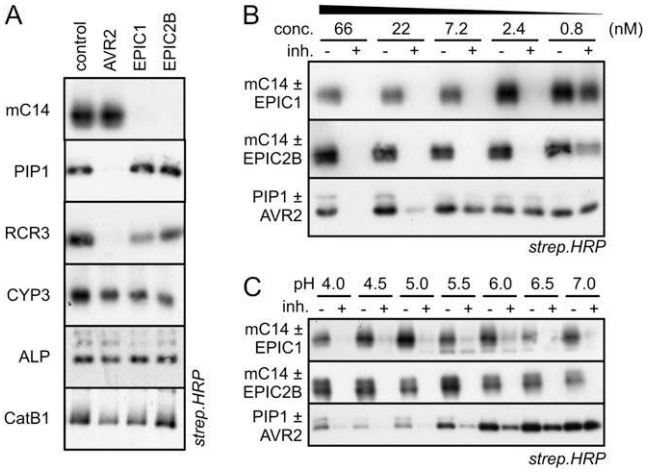

Figure 1. Contrasting selectivity of pathogen-derived inhibitors. A, Extracts from agroinfiltrated *N. benthamiana* leaves overexpressing different proteases (indicated on the left) were preincubated for 30 min with 66 nM AVR2, EPIC1, or EPIC2B. DCG-04 was added after preincubation to label the noninhibited proteases. Biotinylated proteases were visualized on protein blots using streptavidin-HRP. Representatives of at least three independent experiments are shown. B and C, EPIC proteins inhibit at nanomolar concentrations (B), and the inhibition is not pH dependent (C). Protease-containing extracts were incubated with different inhibitor concentrations (B) or at various pH levels (C) for 30 min. DCG-04 was added after preincubation to label the noninhibited proteases. Biotinylated proteins were visualized on protein blots using streptavidin-HRP.

these proteases are active also at nonapoplastic pH (Fig. 1C). Interestingly, inhibition of C14 by EPIC1 and EPIC2B occurs throughout this pH range, in contrast to the inhibition of PIP1 by AVR2, which only occurs at the acidic pH of the apoplast (Fig. 1C).

EPIC Targets C14 in Apoplastic Fluids

To investigate if selective inhibition would also occur in the apoplast, we preincubated apoplastic fluids isolated from tomato with AVR2, EPIC1, or EPIC2B and then labeled them with DCG-04. Like its Arabidopsis ortholog (RD21; Yamada et al. 2001), tomato C14 exists in two active isoforms, due to the presence or absence of a C-terminal granulin domain (Fig. 2A). The intermediate isoform (iC14) carries the granulin domain and is 37 kD, whereas the mature isoform (mC14) is 30 kD and lacks the granulin domain. In the above experiments, we could only analyze mC14, because iC14 tends to precipitate and was not present in extracts from agroinfiltrated leaves. In activity profiles of crude apoplastic fluids, however, iC14 causes a unique 37-kD signal in addition to signals at 30 kD (mC14, CatB1, CatB2, CYP3, and ALP) and 25 kD (PIP1 and RCR3; Shabab et al., 2008). Apoplastic fluids were preincubated with EPICs or AVR2 and then labeled with DCG-04. The biotinylated proteins were purified and analyzed using streptavidin-horseradish peroxidase (HRP) and anti-C14 antibody. Preincubation with both EPIC1 and EPIC2B specifically prevents the biotinylation of both mC14 and iC14 (Fig. 2B, lanes 3 and 4). These data demonstrate that EPICs

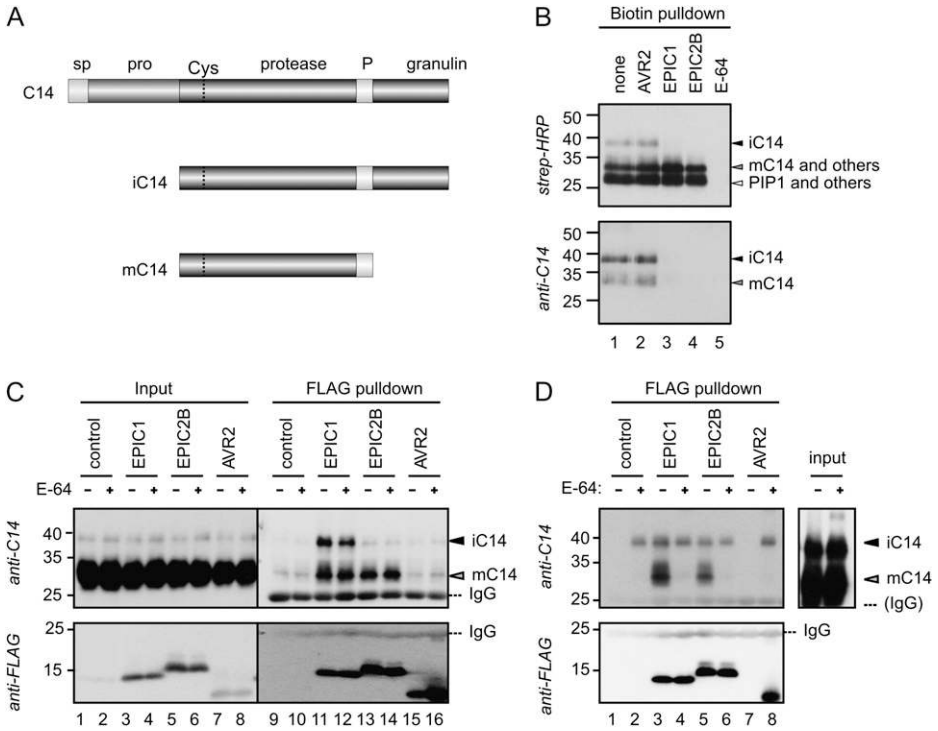

Figure 2. Selective inhibition in apoplastic fluids and physical interaction of C14-EPICs. A, Isoforms of C14. The *C14* gene product contains a signal peptide (sp), an autoinhibitory prodomain (pro), a protease domain with a catalytic Cys (Cys), a Pro-rich domain (P), and a granulin domain. Similar to Arabidopsis RD21 (Yamada et al., 2001), C14 exists in two active forms: intermediate (iC14) and mature (mC14; Shabab et al., 2008). B, Selective inhibition in apoplastic fluids. Tomato apoplastic fluids were preincubated with 1 μM AVR2, EPIC1, or EPIC2B and 200 μM E-64 before adding DCG-04 to label the remaining noninhibited proteases. Biotinylated proteins were purified and detected using streptavidin-HRP (top) and anti-C14 antibody (bottom). The identity of the proteases was determined previously (Shabab et al., 2008). The absence of complete inhibition of PIP1 by AVR2 and EPIC2B is caused by the relatively high PIP1 concentration in these apoplastic fluids when compared with the inhibitor concentrations. C, EPICs physically interact with C14. Extracts of *N. benthamiana* overexpressing C14 were preincubated for 30 min with or without 300 μM E-64 in the absence of DTT. FLAG-tagged EPIC1, EPIC2B, or AVR2 (1 μM) was added and incubated for 30 min. Protein complexes were immunoprecipitated using an anti-FLAG matrix. The matrix was washed and boiled in SDS sample buffer. Eluted proteins were detected on protein blots using C14- and FLAG-specific antibodies. IgG is the light chain anti-FLAG antibody eluted from the anti-FLAG column. D, E-64 prevents the physical interaction of EPICs with C14. Extracts of *N. benthamiana* overexpressing C14 were preincubated for 30 min with or without 300 μM E-64 in the presence of 5 mM DTT. FLAG-tagged EPIC1, EPIC2B, or AVR2 (1 μM) was added and incubated for 30 min. Protein complexes were immunoprecipitated using an anti-FLAG matrix. The pulldown was analyzed as described in C. The presence of iC14 signals in the top panel is due to the fact that iC14 tends to precipitate.

selectively target C14 in apoplastic fluids in the presence of other abundant proteases.

EPIC1 and EPIC2B Physically Interact with C14

We performed coimmunoprecipitations to investigate if there is also a physical interaction between C14 and EPIC1s. Extracts from *Nicotiana benthamiana* leaves transiently overexpressing C14 were preincubated with FLAG-tagged EPIC1, EPIC2B, and AVR2 proteins, and protein complexes were pulled down using anti-FLAG agarose beads. mC14 was coprecipitated with FLAG-EPIC1 and FLAG-EPIC2B but not with FLAG-AVR2 (Fig. 2C, lanes 11–16), demonstrating that mC14 physically and specifically interacts with EPICs but not AVR2.

To test if the EPIC-C14 interaction occurs at the active site, we preincubated C14 with the PLCP inhibitor E-64, which covalently reacts with the catalytic Cys. However, E-64 does not prevent the EPIC-C14 interactions (Fig. 2C, lanes 12 and 14). We realized that it was also difficult to detect C14 activity in these fractions because we did not add the reducing agent dithiothreitol (DTT) to activate PLCPs (data not

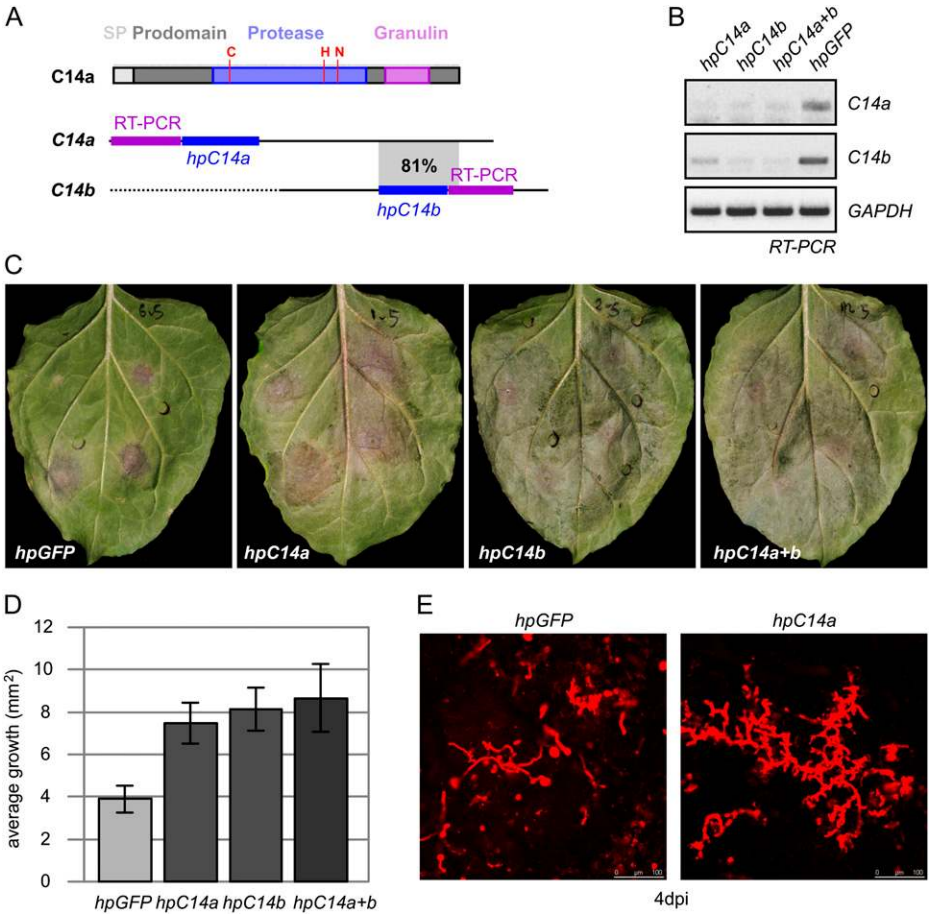

Figure 3. *C14* silencing enhances susceptibility for *P. infestans*. A, Fragments used for silencing and RT-PCR. *C14a* encodes a full-length C14 protein, whereas *C14b* lacks the 5′ half of the cDNA. The C14 protein consists of a signal peptide (SP), a prodomain, a protease domain with three catalytic residues (red), and a granulin domain with Cys residues (purple). *C14a* and *C14b* share a fragment with 81% nucleotide identity (gray). Fragments for silencing and RT-PCR are indicated in blue and purple, respectively. B, Transcript levels in leaves upon agroinfiltration of hairpin constructs. *Agrobacterium tumefaciens* carrying binary plasmids containing 35S-driven hairpin fragments for GFP, C14a, or C14b were infiltrated into adult leaves of *N. benthamiana*. Total RNA was extracted at 4 dpi and used as a template for RT-PCR using gene-specific primers for *C14* and *GAPDH*. C, Symptoms of hairpin-treated *N. benthamiana* leaves upon infection with *P. infestans*. Leaves of *N. benthamiana* were agroinfiltrated with *hpGFP*, *hpC14a*, *hpC14b*, or both *hpC14a* + *hpC14b* and 4 d later inoculated with four droplets each containing zoospores of *P. infestans* 88069td. Photographs were taken at 5 dpi. D, Increased growth of *P. infestans* in *hpC14*-treated plants. Plants were infected as described in C with RFP-expressing *P. infestans* 88069td. The infected area was measured at 5dpi by fluorescence microscopy and ImageJ. Error bars indicate SE of five independent biological assays. Student's *t* test compared the findings with the *hpGFP* control: $P = 0.017$ (*hpC14a* + *hpC14b*), $P = 0.008$ (*hpC14a*), and $P = 0.004$ (*hpC14b*). E, Enhanced hypha growth of RFP-expressing *P. infestans* on *hpC14*-treated leaves. Leaves of *N. benthamiana* were infected as described in C, and photographs were taken at 2 dpi using confocal microscopy. Bars = 100 μm.

shown). Since E-64 can only react with active proteases, the absence of DTT prevents the binding of E-64 to C14. Therefore, binding and pulldown experiments were repeated in the presence of DTT. Also in the presence of DTT, mC14 coprecipitates with FLAG-EPIC1 and FLAG-EPIC2B (Fig. 2D, lanes 3 and 5). However, in the case of the AVR2 control, the FLAG-AVR2 signal disappears (Fig. 2D, lane 7), presumably because the C14 activity degrades FLAG-AVR2. Indeed, adding E-64 stabilizes FLAG-AVR2 (Fig. 2D, lane 8). This experiment demonstrates that AVR2 does not inhibit C14 and that FLAG-AVR2 becomes a substrate for the protease. Importantly, in the presence of DTT and E-64, there is no interaction between C14 and EPICs (Fig. 2D, lanes 4 and 6). Thus, EPICs physically interact with the C14 protease domain, and this interaction occurs under both reducing and oxidative conditions and can be prevented by labeling the active site with E-64.

C14 Silencing Enhances Susceptibility to *P. infestans* in *N. benthamiana*

To investigate a possible role of C14 in defense against *P. infestans*, we performed transient silencing experiments in *N. benthamiana*, a useful model host for *P. infestans*. Using the granulin domain of tomato C14 as a template for tBLAST searches, we identified in The Institute for Genomic Research cDNA database of *N. benthamiana* two *C14* orthologs (TC7740 [*C14a*] and EST748747 [*C14b*]), which share sufficient nucleotide identity to expect cosilencing (T. Shindo and R.A.L. van der Hoorn, unpublished data). Fragments of two of these genes were used to construct 35S-driven hairpin (hp) constructs of *C14a* and *C14b* (Fig. 3A). *hpGFP* was used as a negative control for silencing (Johansen and Carrington, 2001). Agroinfiltration of the *hpC14* constructs results in reduced *C14* transcript levels at 4 d postinfiltration (dpi; Fig. 3B). Although cosilencing occurs, we found that *hpC14a* predominantly suppresses *C14a* transcript levels, whereas *hpC14b* suppresses *C14b* transcript levels (Fig. 3B).

Leaves treated with *hpC14* and *hpGFP* constructs were used for *P. infestans* infection assays. Importantly, in contrast to *hpGFP*-treated plants, *hpC14*-treated leaves become heavily infected, showing increased mycelium growth at 3 dpi and intense sporulation at 5 dpi (Fig. 3C). Quantification of infected areas demonstrated a significantly enhanced susceptibility that was identical for *hpC14a*, *hpC14b*, and *hpC14a* + *hpC14b* treatments (Fig. 3D), consistent with the cosilencing of the two *C14* genes.

To investigate differences at earlier stages during infection, we monitored the growth of *P. infestans* strain 88609 expressing the cytosolic red fluorescent protein (RFP; Whisson et al., 2007) on *hpC14*-treated leaves. Microscopic studies revealed a marked increase in the hyphal growth of *P. infestans* on *C14*-silenced leaves when compared with the negative control leaves starting from day 2 after inoculation (Fig. 3E). Taken together, these data demonstrate that *C14* silencing enhances susceptibility to *P. infestans*.

Natural Variation of C14 in Wild Potato Species

We previously found that AVR2 targets RCR3 and PIP1, which are both under diversifying selection in wild tomato species (Shabab et al., 2008). This is consistent with the hypothesis of an arms race between

A

species	#n	accession	clones/allele A	B	C	D	E	F	G	#
S.demissum	6n	BGRC053643	3	-	-	-	-	3	-	**6**
		BGRC010022	4	-	-	2	-	-	-	**6**
S.verrucosum	2n	BCRC008255	-	-	-	-	-	5	-	**6**
		BGRC008246	-	-	-	-	-	6	-	**6**
		BGRC008250	-	-	-	-	-	5	-	**6**
S.stoloniferum	4n	BGRC007230	-	-	-	-	5	-	-	**6**
		BGRC007229	-	3	-	-	-	-	3	**6**
S.tuberosum	4n	NCBI	-	-	+	-	-	-	-	-

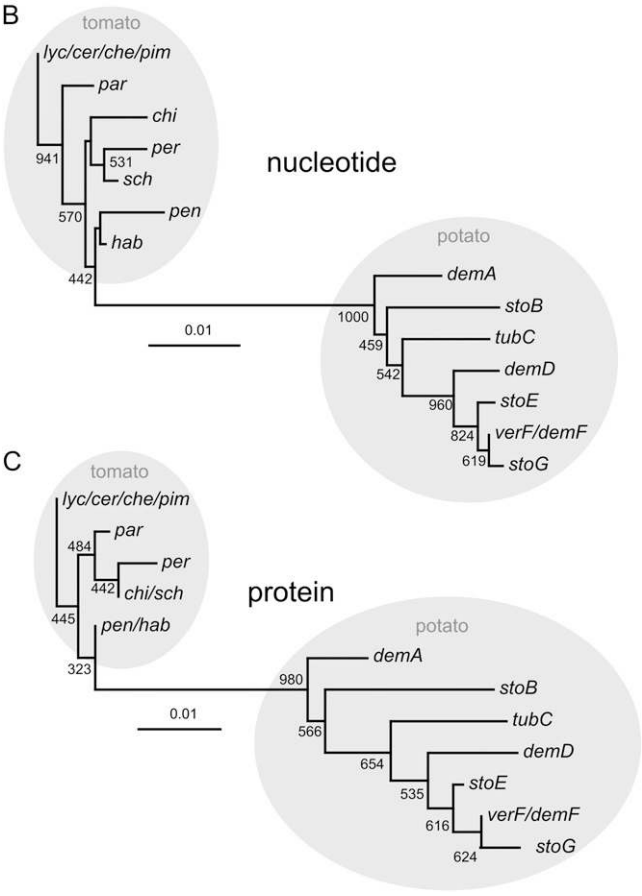

Figure 4. Distribution of *C14* alleles in tomato and potato. A, Occurrence of *C14* alleles in wild potato species. Six *C14* genes were cloned from each accession and sequenced. The frequency of alleles A to G is summarized for the different accessions. The ploidy levels (n) of the species are indicated. B, Phylogenetic tree of *C14* at the nucleotide level. Tomato *C14* was used as an outgroup. Numbers indicate the frequency of presented branches over 1,000 bootstraps. C, Phylogenetic tree of C14 at the protein level. Tomato C14 was used as an outgroup. Numbers indicate the frequency of presented branches over 1,000 bootstraps.

proteases and their inhibitors at the plant-pathogen interface (Misas-Villamil and van der Hoorn, 2008). In contrast to *RCR3* and *PIP1*, however, *C14* is under conservative selection in tomato, evident from the fact that only a few variant codons change the encoded amino acids (Shabab et al., 2008). Since wild tomato is not the natural host of *P. infestans*, we looked for natural variation of *C14* in *Solanum demissum*, *Solanum verrucosum*, and *Solanum stoliniferum*, three wild potato species that are known to be the natural hosts of *P. infestans* in its center of origin in Tolucca Valley, Mexico (Debener et al., 1990; Grünwald and Flier, 2005).

Several accessions of these wild potato species were grown, and mRNA from leaves was used as a template for reverse transcription (RT)-PCR with primers for tomato *C14*. Amplified products were cloned, and six independent clones per plant were sequenced. Sequences were aligned, and polymorphic nucleotides were quality checked using the trace data and by comparing the clones. A total of six new *C14* alleles were identified in addition to the *C14* allele of cultivated potato deposited in the National Center for Biotechnology Information database (AJ245924; Fig. 4A). Several potato accessions contained two alleles, consistent with their ploidy level. Two alleles were identified from both *S. demissum* accessions (hexaploid) and one of the two *S. stoliniferum* accessions (tetraploid). Only one allele was identified in the diploid *S. verrucosum*. Allele F is common to *S. verrucosum* and also found in *S. demissum*, whereas the other alleles were only found in one of the species. The *C14* alleles from wild potato are also distinct from the *C14* allele of cultivated potato present in the National Center for Biotechnology Information database.

Phylogenetic analysis revealed that the potato *C14* alleles are different from the tomato *C14* alleles, both at the protein and nucleotide levels (Fig. 4, B and C). Comparison of phylogenetic trees shows that the branch length of *C14* in tomato contracts at the protein level when compared with the nucleotide level (Fig. 4, B and C), consistent with the conservative selection on tomato *C14*. Branch lengths of potato *C14s*, however, expand at the protein level (Fig. 4, B and C), suggesting that most of the nucleotide polymorphisms in potato *C14s* cause amino acid changes.

C14 Is under Diversifying Selection in Wild Potato

To investigate if the *C14* sequences are under selective pressure, we calculated the ratio of the rate of nonsynonymous substitutions (Ka) to the rate of synonymous substitutions (Ks) in pairwise comparisons of all combinations of tomato and potato *C14* alleles (Table I; Nei and Gojobori, 1986; Zhang et al. 2006). Importantly, the Ka/Ks ratio for tomato alleles (0.07 ± 0.04) is significantly different when compared with the Ka/Ks ratio of the potato alleles (0.40 ± 0.23; Table I). Ka/Ks ratios in intraspecies comparisons are intermediate. These data indicate that *C14* is under contrasting selection pressure in tomato and potato.

We next performed the maximum likelihood method implemented in the Phylogenetic Analysis by Maximum Likelihood package on the potato *C14* sequences to determine the degree to which they are under diversifying selection (Yang, 2007). A likelihood ratio test was conducted comparing the null model (M7) with the alternative model (M8), revealing a 95% probability that potato *C14* is under diversifying selection, compared with 10% probability for tomato *C14*. Thus, in contrast to tomato *C14*, potato *C14* is under diversifying selection.

The probability that variant codons are under positive selection was inferred by Bayes Empirical Bayes analysis (Yang et al., 2005) and is summarized in Figure 5A. Bayes Empirical Bayes analysis showed that one codon in tomato *C14* and four codons in potato *C14* are under positive selection. Codon 195 in tomato *C14* has 82% probability to be under positive selection and

Table I. *Ka/Ks ratio of pairwise comparisons of all tomato and potato C14s*

Entries in bold and italics indicate Ka/Ks > 0.3, and entries in bold indicate Ka/Ks < 0.1. * Ks = 0. NA, Not analyzed.

	Ka/Ks	Tomato Alleles							Potato Alleles						
		lyc	*chi*	*pen*	*hab*	*per*	*sch*	*par*	*C*	*F*	*E*	*G*	*B*	*A*	*D*
Tomato alleles	*lyc*	NA	**0.09**	**0.03**	**0.09**	0.17	0.14	**0.09**	0.25	0.24	0.21	0.25	0.26	0.17	0.25
	chi		NA	**0.03**	**0.06**	**0.04**	**0.00**	**0.04**	0.22	0.24	0.21	0.25	0.25	0.15	0.25
	pen			NA	**0.00**	**0.06**	**0.03**	**0.06**	0.24	0.22	0.19	0.24	0.24	0.14	0.24
	hab				NA	0.14	**0.06**	**0.09**	0.29	0.27	0.23	0.29	0.29	0.17	0.29
	per					NA	**0.09**	**0.09**	0.25	0.27	0.24	0.29	0.29	0.18	0.25
	sch						NA	**0.09**	0.25	0.27	0.23	0.29	0.29	0.20	0.29
	par							NA	0.25	0.27	0.24	0.29	0.29	0.20	0.29
Potato alleles	*C*								NA	0.20	0.21	0.24	***1.16***	***0.33***	0.24
	F									NA	0.28	*	***0.52***	0.19	***0.43***
	E										NA	***0.57***	***0.40***	0.19	***0.38***
	G											NA	***0.57***	0.22	***0.57***
	B												NA	***0.46***	***0.48***
	A													NA	0.25
	D														NA

encodes either Arg or Lys. Codons 199 and 221 in potato *C14* have 86% and 88% probability, respectively, to be under positive selection, causing Gln-Glu and Ser-Thr polymorphisms, respectively. Codons 245 and 323 in potato *C14* both have a 98% probability to be under positive selection. The residues encoded by these codons are remarkably diverse: Lys, Thr, and Val for codon 245 and Lys, Asn, and Asp for codon 323.

Since codons 245 and 323 encode more than two residues, we investigated if these codons mutated independently from each other. The sequences of codon 245 are ACA, GTA, and AAA and therefore represent independent mutations. The sequences of codon 323 are AAA, AAC, and GAC, which can be a result of consecutive mutations. However, when plotted onto the phylogenetic tree, the variant codons map to distinct branches (Fig. 5B), suggesting that these codons have also evolved independently. Thus, residues 245 and 323 are probably caused by homoplasmic mutations that emerged independently.

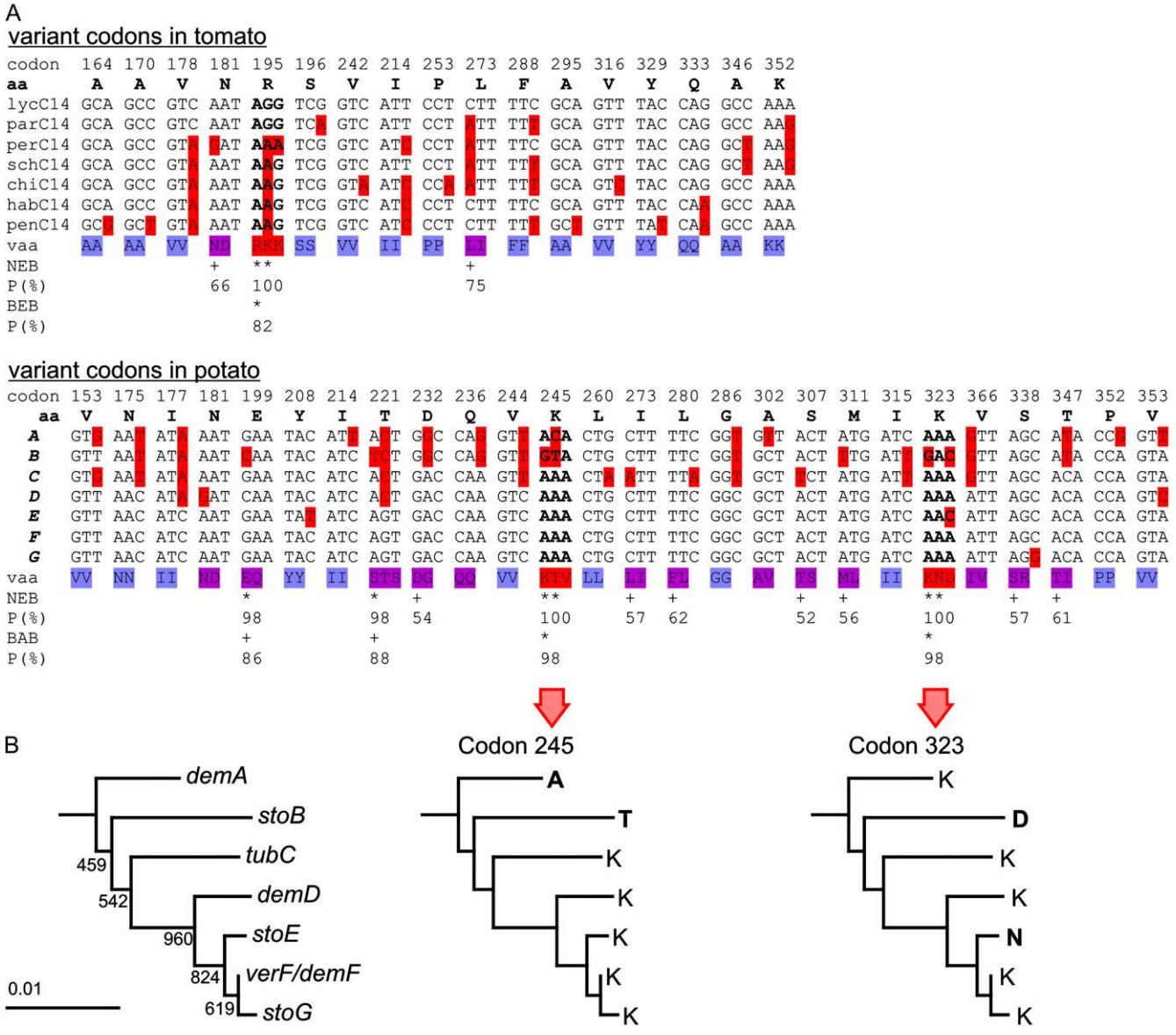

Figure 5. Potato *C14* is under diversifying selection. A, Variant codons in the potato and tomato *C14* protease domain. The codon numbering is from the start codon. The amino acid (aa) at the top represents the residue encoded by the codon in cultivated tomato or potato. Codons at variant positions are summarized with the variant nucleotide indicated in red. The hypervariable codons are indicated in boldface. The variant amino acids (vaa) are indicated in blue (identical), purple (similar), or red (variable). The probability scores for Naive Empirical Bayes (NEB) and Bayes Empirical Bayes (BEB) scores are indicated ($^{+}$ $P > 50\%$, * $P > 95\%$, ** $P > 99\%$). B, Occurrence of amino acids under diversifying selection within the nucleotide phylogenetic tree of potato. The amino acids encoded by codons 245 and 323 were plotted in the phylogenetic tree of potato *C14*.

DISCUSSION

We discovered that the solanaceous C14 protease is a novel target of the apoplastic effector proteins EPIC1 and EPIC2B of *P. infestans*. C14 is inhibited by EPICs under a wide range of conditions, and *C14* silencing increases susceptibility to *P. infestans*. C14 is under conservative selection in tomato but under diversifying selection in wild potato species that are the natural hosts of *P. infestans*. These observations indicate that C14 is a protease that contributes to defense against *P. infestans*, and as a counterdefense mechanism, *P. infestans* secretes EPICs during infection to inhibit C14 in the apoplast. Consequently, C14 became involved in a coevolutionary arms race, a process that has left imprints in the potato C14 sequences. However, this only occurred in plants that are a natural host for *P. infestans*.

Here, we show that C14 is involved in immunity and targeted by pathogen effectors. C14 is a highly conserved protease that occurs throughout the plant kingdom. C14-like proteases are characterized by a unique, C-terminal granulin-like domain that shares homology with animal growth hormones that are released upon wounding (Bateman and Bennett, 1998). The tomato C14 is relatively abundant and has been well studied under the names TDI-65, CYP1, and SENU1. *C14* is known to be transcriptionally induced by heat, cold, drought, and senescence (Schaffer and Fischer, 1988, 1990; Drake et al., 1996; Harrak et al., 2001). The potato ortholog of C14 has also been called CYP1 and is transcriptionally induced in resistant potato cultivars early during infection with *P. infestans* (Avrova et al., 1999). Transcript levels of potato *C14* are also up-regulated during compatible interactions with *P. infestans* (Supplemental Fig. S2; Haas et al., 2009). The Arabidopsis ortholog of C14 is named RD21; it accumulates in the vacuole and in vesicles and can act as a peptide ligase (Hayashi et al., 2001; Yamada et al., 2001; Wang et al., 2008).

EPICs are expressed at early biotrophic stages during tomato and potato infection (Tian et al., 2007; Haas et al., 2009). Most likely, secreted EPIC proteins encounter C14 proteins surrounding the hypha, since C14 is present in the tomato apoplast (Shabab et al., 2008). EPICs might protect the hypha against proteolytic damage imposed by C14 and other secreted proteases. Alternatively, the EPICs could interfere with potential immune signaling functions of the targeted proteases.

Besides C14, EPICs also inhibit PIP1 (Tian et al., 2007) and RCR3 (Song et al., 2009). However, in contrast to EPIC-PIP1 and EPIC-RCR3 interactions, the EPIC-C14 interactions sustain long DCG-04 labeling times, indicating that EPIC-C14 is a stronger interaction based on higher affinity. One possibility is that, when secreted into the apoplast by the extending hypha, the EPICs will first inhibit C14, and the remaining EPIC proteins would target PIP1 and RCR3. This selectivity suggests that at high EPIC concentrations (e.g. at the hyphal tip surface, where EPIC secretion most likely occurs), C14, PIP1, and RCR3 are inhibited, whereas at lower EPIC concentrations (e.g. at the host cell surface), EPICs may only inhibit C14. A better understanding of the cellular dynamics of the expression and secretion of the PLCP and their inhibitors is needed to understand this complex interplay.

The selectivity and properties of the EPIC inhibitors of the oomycete *P. infestans* are notably different from those of the fungal apoplastic effector AVR2. In contrast to the observation that EPICs inhibit C14 at wide pH ranges, AVR2 preferentially inhibits PIP1 and RCR3 at apoplastic pH. *C. fulvum* is a strictly biotrophic fungal pathogen that only resides in the apoplast, whereas *P. infestans* is a hemibiothropic oomycete pathogen that initially establishes a biotrophic interaction but then colonizes dead host tissues at a later stage during infection. The contrasting selectivity and properties of EPICs and AVR2 might be associated with these different lifestyles. Alternatively, effectors with different inhibitory selectivity remain to be discovered from these pathogens.

Interestingly, C14 is also targeted by other plant pathogen effectors besides the EPICs of *P. infestans*. In addition to strong interactions with PIP1 and RCR3, AVR2 was found to have weak physical interaction with tomato C14 (van Esse et al., 2008). Furthermore, we discovered that *Pseudomonas syringae* produces a protease inhibitor (named RIP1) that selectively targets tomato C14 and Arabidopsis RD21, similar to the selectivity of EPICs (F. Kaschani and R.A.L. van der Hoorn, unpublished data). C14 was also found to interact with another effector protein of *P. infestans*, the host translocated RXLR effector AvrBlb2 (T. Bozkurt, S. Schornack, J. Win, and S. Kamoun, unpublished data; Oh et al., 2009). This indicates that different pathogen effectors target C14 and implies that C14 may also play a general role in immunity to bacterial and fungal diseases.

C14 is under diversifying selection in wild potato species and under conservative selection in wild tomato species. The contrasting selection pressure is clear from sequence analysis using both the approximate and maximum likelihood methods, and we found two sites with putative homoplasmic mutations. The contrasting selection pressure suggests that in natural populations, C14 might be under stronger selective pressure from potato pathogens (e.g. *P. infestans*) than from tomato pathogens. Further studies on the interactions of the effectors with the variant versions of C14 might reveal an exciting example of multicomponent molecular arms races at the plant-pathogen interface.

MATERIALS AND METHODS

Plant Growth

All plants were grown in a climate chamber under a 14-h light regime at 18°C (night) and 22°C (day). Four- to 6-week-old plants were used for experiments.

Cloning of Wild Potato C14 Alleles

Total RNA from wild potato species (*Solanum demissum*, *Solanum verrucosum*, and *Solanum stoloniferum*) was isolated using the RNA extraction kit from Qiagen. First-strand cDNA was then synthesized using the SuperScript II reverse transcriptase from Invitrogen (www.invitrogen.com) according to the manufacturer's suggestions. Potato (*Solanum tuberosum*) C14 cDNAs were amplified by PCR with High Fidelity Taq from Roche (www.roche.com) using LeC14-specific primers r057 (forward, 5′-AGCTGGATCCTCAAGAACT-GCTCTTCTTTCCTCC-3′) and r110 (reverse, 5′-ATGGCCTCGAGCAGCT-CAACTCTCACCATATCC-3′). The PCR products were purified using the PCR purification kit from Qiagen and then cloned by A/T cloning into the pGEM-T vector (Promega).

EPIC1, EPIC2B, and AVR2

Expression of AVR2, EPIC1, and EPIC2B in *Escherichia coli* was conducted as described previously (Tian et al., 2007; Shabab et al., 2008). Protein purities were checked on 17% protein gels by staining with Coomassie Brilliant Blue or by silver staining, and proteins were quantified using the Bradford assay (Bio-Rad) following the manufacturer's guidelines.

Inhibition Assays with Agroinfiltrated Proteases

Tomato (*Solanum lycopersicum*) proteases were overexpressed by agroinfiltration as described earlier (Shabab et al., 2008). Apoplastic fluids or total extracts from agroinfiltrated *Nicotiana benthamiana* were isolated at 5 dpi. In a total volume of 400 μL, 40 μL of extract was preincubated in 50 mM NaAc, pH 5, 1 mM L-Cys, with or without AVR2, EPIC1, or EPIC2B or 10 μM E-64 for 30 min at room temperature. DCG-04 was added to a final concentration of 2 μM, and the labeling was performed for another 5 h at room temperature. Proteins were precipitated by adding 1 mL of ice-cold acetone and centrifugation (1 min, 16,000*g*). Pellets were dissolved in SDS gel loading buffer. Detection of biotinylated proteins was done as described previously using streptavidin-HRP polymer (Sigma-Aldrich; van der Hoorn et al., 2004).

Activity-Based Profiling on Tomato Extracts

Apoplastic fluids were isolated by vacuum infiltration of tomato leaves as described earlier (Shabab et al., 2008). One milliliter of tomato apoplastic fluids was diluted into a 2-mL total volume containing 50 mM NaOAc, pH 5, and 10 mM DTT. These extracts were preincubated for 30 min at room temperature with 1 μM AVR2, EPIC1, or EPIC2B or 200 μM E-64 and then labeled for 90 min with 5 μM DCG-04. The samples were desalted into phosphate-buffered saline (50 mM $NaPO_4$, pH 7.5, and 150 mM NaCl) using 10DG desalting columns (Bio-Rad). After the buffer exchange, SDS was added to the eluted fractions to a final concentration of 0.2% SDS, followed by the addition of the equivalent of 100 μL of phosphate-buffered saline-washed avidin beads (Sigma). After 1 h of incubation, the beads were collected by gentle centrifugation and washed four times with 1% SDS. The beads were heated with SDS sample buffer, and the eluted protein mix was analyzed by western blotting using streptavidin-HRP and anti-C14 antibody.

Western-Blot Analysis

Western-blot analysis was performed as described for detection of biotinylated proteins using C14 and PIP1 antibodies (Tian et al., 2007) followed by detection with HRP-conjugated anti-rabbit antibodies (Amersham).

C14 antibodies were raised in rabbits using peptides 5′-DTEEDYPY-KERNGVC-3′ and 5′-DQYRKNAKVVKIDSYC-3′ (Eurogentec) and tested on extracts with and without C14.

Immunoprecipitation

For coimmunoprecipitations, 100 μL of C14-containing extract was mixed with 7 mL of 50 mM NaOAc, pH 5, in the presence (5 mM; PLCP activation) or absence of DTT. Aliquots (500 μL) of this master mix were then preincubated with or without 300 μM E-64 for 30 min at pH 5 and then incubated with 1 μM FLAG-tagged EPIC or AVR2 proteins (30 min). Then, the pH was increased to pH 7.6 by adding 66 μL of 10× Tris-buffered saline to allow capture of the FLAG-tagged proteins on the anti-FLAG M2 affinity matrix (Sigma). The matrix was washed three times with Tris-buffered saline containing 0.2% Tween 20 (Sigma) and eluted with 30 μL of gel-loading buffer. Eluates were analyzed on western blots with C14 and M2 FLAG antisera (Sigma).

Phylogenetic Analysis

The tomato C14 sequences were taken from Shabab et al. (2008). Tomato and potato sequences were loaded into ClustalX2.09 (Larkin et al., 2007) and aligned following the guidelines of Hall (2004). The unrooted consensus trees from 1,000 bootstrap trees were then generated, and the resulting files were exported to Adobe Illustrator (www.adobe.com) for further editing. Ka/Ks values were calculated using the method of Nei and Gojobori (1986) as implemented in the KaKs_Calculator (Zhang et al., 2006).

Infection Assays

For each silencing construct, three leaves of a 6-week-old *N. benthamiana* plant were agroinfiltrated with strains carrying hairpin silencing constructs. Infections were done as described previously (Song et al., 2009). *P. infestans* infection assays on *N. benthamiana* were performed by droplet inoculations of zoospore solutions on detached leaves as described (Vleeshouwers et al., 1999). *P. infestans* isolate 88069td expressing the RFP variant tdTomato was used to visualize pathogen colonization (obtained from S. Whisson). 88069td (100,000 spores mL^{-1}) was inoculated on four different spots of 4-week-old *N. benthamiana* leaves. Two days later, leaf discs encompassing the droplet and surrounding area were mounted in water and inspected on a Leica SP5 confocal microscope using an excitation wavelength of 561 nm and detector settings for mRFP fluorescence. *P. infestans* 88069td growth efficiency was quantified using the ImageJ program by measuring the average total area of the red-fluorescing hypha monitored at 5 dpi in five independent biological assays.

Construction of *hpC14* Constructs

A PCR fragment generated from the first intron of Arabidopsis (*Arabidopsis thaliana*) At5g15070 was amplified with primers 5′-GTGCGGATCCTGATGT-CAGAAGAGTAAGG-3′ and 5′-CTACGAGCTCATAAGCTTATCTAGAC-AGC-3′ and cloned into pGEM-T using *Xho*I and *Bam*HI to construct pFK29. Sense-orientated fragments of *C14a* and *C14b* were amplified by PCR using primers 5′-GATCCCATGGTCTGAACAAGTTTGCTGATATGAG-3′, 5′-GAT-CGGATCCGTCCACCATCACAGCCAGTATTG-3′, 5′-GATCCCATGGACC-CCCTCCACCACCTTCTCCG-3′, and 5′-GATCGGATCCTAACTTGTATTTGG-CTATTCTTC-3′ and cloned into pFK26 using *Nco*I-*Bam*HI, resulting in pTS40 and pTS42, respectively. Antisense-orientated fragments of *C14a* and *C14b* were amplified by PCR using primers 5′-GATCCTCGAGCTGCAGTCTGAACAA-GTTTGCTGATATGAG-3′, 5′-GATCTCTAGAGTCCACCATCACAGCCAGTA-TTG-3′, 5′-GATCCTCGAGCTGCAGACCCCCTCCACCACCTTCTCCG-3′, and 5′-GATCTCTAGATAACTTGTATTTGGCTATTCTTC-3′ and cloned into pFK29 using *Pst*I and *Xba*I, resulting in pTS41 and pTS43, respectively. The antisense fragments of pTS41 and pTS43 were cloned into pTS40 and pTS42, respectively, using *Bam*HI and *Pst*I, resulting in pTS50 and pTS51, respectively. This insert was cloned into the binary vector pTP5 (Shabab et al., 2008) using *Hin*dIII and *Eco*RI, yielding binary 35S-driven hairpin C14 constructs pTS54 and pTS55 for *C14a* and *C14b*, respectively.

RT-PCR

Total RNA was isolated from tissues frozen in liquid nitrogen using the RNeasy Plant Mini Kit (Qiagen) according to the manufacturer's guidelines. DNase treatment was done before the RNA concentration was measured. cDNA was synthesized using SuperScript II reverse transcriptase and oligo (dT) primers. PCR was performed with gene-specific primers for *C14a* (5′-GATCGGATCCGTTACTGAAAAATGGGAAGCACAC-3′ and 5′-GAT-CGAATTCCCAACCAAATGATCTGAGTTTGAC-3′), *C14b* (5′-GATCGGAT-CCGGTGGACGAAACTCTGAAATGG-3′ and 5′-GATCGAATTCTTTATTC-AAGAATGTACACAGCG-3′), and *GAPDH* (5′-ATGGCTTCTCATGCAGC-TTT-3′ and 5′-ATCCTGTGGTCTTGGGAGTG-3′).

Sequence data from this article can be found in the GenBank/EMBL data libraries under accession numbers HQ426918 to HQ426927.

Supplemental Data

The following materials are available in the online version of this article.

Supplemental Figure S1. Activities of tomato PLCPs upon agroinfiltration.

Supplemental Figure S2. Potato C14 is transcriptionally induced during *P. infestans* infection.

ACKNOWLEDGMENTS

We thank Christiane Gebhardt for providing wild potato accessions, Steve Whisson for providing the *P. infestans* 88069td strain, and Anja Höger and Bikram Pandey for technical support.

Received April 18, 2010; accepted October 11, 2010; published October 12, 2010.

LITERATURE CITED

Avrova AO, Stewart HE, De Jong WD, Heilbronn J, Lyon GD, Birch PR (1999) A cysteine protease gene is expressed early in resistant potato interactions with *Phytophthora infestans*. Mol Plant Microbe Interact **12:** 1114–1119

Bateman A, Bennett HPJ (1998) Granulins: the structure and function of an emerging family of growth factors. J Endocrinol **158:** 145–151

Bishop JG, Dean AM, Mitchell-Olds T (2000) Rapid evolution in plant chitinases: molecular targets of selection in plant-pathogen coevolution. Proc Natl Acad Sci USA **97:** 5322–5327

Bishop JG, Ripoll DR, Bashir S, Damasceno CM, Seeds JD, Rose JK (2005) Selection on glycine beta-1,3-endoglucanase genes differentially inhibited by a Phytophthora glucanase inhibitor protein. Genetics **169:** 1009–1019

Damasceno CM, Bishop JG, Ripoll DR, Win J, Kamoun S, Rose JK (2008) Structure of the glucanase inhibitor protein (GIP) family from Phytophthora species suggests coevolution with plant endo-beta-1,3-glucanases. Mol Plant Microbe Interact **21:** 820–830

Debener T, Salamini F, Gebhardt C (1990) Phylogeny of wild and cultivated *Solanum* species based on nuclear restriction fragment length polymorphisms (RFLPs). Theor Appl Genet **79:** 360–368

Dixon MS, Golstein C, Thomas CM, van Der Biezen EA, Jones JD (2000) Genetic complexity of pathogen perception by plants: the example of *Rcr3*, a tomato gene required specifically by *Cf-2*. Proc Natl Acad Sci USA **97:** 8807–8814

Drake R, John I, Farrell A, Cooper W, Schuch W, Grierson D (1996) Isolation and analysis of cDNAs encoding tomato cysteine proteases expressed during leaf senescence. Plant Mol Biol **30:** 755–767

Ferreira RB, Monteiro S, Freitas R, Santos CN, Chen Z, Batista LM, Duarte J, Borges A, Teixeira AR (2007) The role of plant defence proteins in fungal pathogenesis. Mol Plant Pathol **8:** 677–700

Greenbaum D, Medzihradszky KF, Burlingame A, Bogyo M (2000) Epoxide electrophiles as activity-dependent cysteine protease profiling and discovery tools. Chem Biol **7:** 569–581

Grünwald NJ, Flier WG (2005) The biology of *Phytophthora infestans* at its center of origin. Annu Rev Phytopathol **43:** 171–190

Haas BJ, Kamoun S, Zody MC, Jiang RH, Handsaker RE, Cano LM, Grabherr M, Kodira CD, Raffaele S, Torto-Alalibo T, et al (2009) Genome sequence and analysis of the Irish potato famine pathogen *Phytophthora infestans*. Nature **461:** 393–398

Hall BG (2004) Phylogenetic Trees Made Easy: A How-To Manual, Ed 2. Sinauer Associates, Sunderland, MA

Harrak H, Azelmat S, Baker EN, Tabaeizadeh Z (2001) Isolation and characterization of a gene encoding a drought-induced cysteine protease in tomato (*Lycopersicon esculentum*). Genome **44:** 368–374

Hayashi Y, Yamada K, Shimada T, Matsushima R, Nishizawa NK, Nishimura M, Hara-Nishimura I (2001) A proteinase-storing body that prepares for cell death or stresses in the epidermal cells of Arabidopsis. Plant Cell Physiol **42:** 894–899

Hogenhout SA, Van der Hoorn RAL, Terauchi R, Kamoun S (2009) Emerging concepts in effector biology of plant-associated organisms. Mol Plant Microbe Interact **22:** 115–122

Johansen LK, Carrington JC (2001) Silencing on the spot: induction and suppression of RNA silencing in the *Agrobacterium*-mediated transient expression system. Plant Physiol **126:** 930–938

Larkin MA, Blackshields G, Brown NP, Chenna R, McGettigan PA, McWilliam H, Valentin F, Wallace IM, Wilm A, Lopez R, et al (2007) Clustal W and Clustal X version 2.0. Bioinformatics **23:** 2947–2948

Misas-Villamil JC, van der Hoorn RA (2008) Enzyme-inhibitor interactions at the plant-pathogen interface. Curr Opin Plant Biol **11:** 380–388

Nei M, Gojobori T (1986) Simple methods for estimating the numbers of synonymous and nonsynonymous nucleotide substitutions. Mol Biol Evol **3:** 418–426

Oh SK, Young C, Lee M, Oliva R, Bozkurt TO, Cano LM, Win J, Bos JI, Liu HY, van Damme M, et al (2009) In planta expression screens of *Phytophthora infestans* RXLR effectors reveal diverse phenotypes, including activation of the *Solanum bulbocastanum* disease resistance protein Rpi-blb2. Plant Cell **21:** 2928–2947

Rooney HC, Van't Klooster JW, van der Hoorn RA, Joosten MH, Jones JD, de Wit PJ (2005) Cladosporium Avr2 inhibits tomato Rcr3 protease required for *Cf-2*-dependent disease resistance. Science **308:** 1783–1786

Rose JK, Ham KS, Darvill AG, Albersheim P (2002) Molecular cloning and characterization of glucanase inhibitor proteins: coevolution of a counterdefense mechanism by plant pathogens. Plant Cell **14:** 1329–1345

Schaffer MA, Fischer RL (1988) Analysis of mRNAs that accumulate in response to low temperature identifies a thiol protease gene in tomato. Plant Physiol **87:** 431–436

Schaffer MA, Fischer RL (1990) Transcriptional activation by heat and cold of a thiol protease gene in tomato. Plant Physiol **93:** 1486–1491

Shabab M, Shindo T, Gu C, Kaschani F, Pansuriya T, Chintha R, Harzen A, Colby T, Kamoun S, van der Hoorn RA (2008) Fungal effector protein AVR2 targets diversifying defense-related Cys proteases of tomato. Plant Cell **20:** 1169–1183

Song J, Win J, Tian M, Schornack S, Kaschani F, Ilyas M, van der Hoorn RA, Kamoun S (2009) Apoplastic effectors secreted by two unrelated eukaryotic plant pathogens target the tomato defense protease Rcr3. Proc Natl Acad Sci USA **106:** 1654–1659

Tian M, Benedetti B, Kamoun S (2005) A second Kazal-like protease inhibitor from *Phytophthora infestans* inhibits and interacts with the apoplastic pathogenesis-related protease P69B of tomato. Plant Physiol **138:** 1785–1793

Tian M, Huitema E, Da Cunha L, Torto-Alalibo T, Kamoun S (2004) A Kazal-like extracellular serine protease inhibitor from *Phytophthora infestans* targets the tomato pathogenesis-related protease P69B. J Biol Chem **279:** 26370–26377

Tian M, Win J, Song J, van der Hoorn R, van der Knaap E, Kamoun S (2007) A *Phytophthora infestans* cystatin-like protein targets a novel tomato papain-like apoplastic protease. Plant Physiol **143:** 364–377

van den Burg HA, Harrison SJ, Joosten MH, Vervoort J, de Wit PJ (2006) *Cladosporium fulvum* Avr4 protects fungal cell walls against hydrolysis by plant chitinases accumulating during infection. Mol Plant Microbe Interact **19:** 1420–1430

van der Hoorn RA, Leeuwenburgh MA, Bogyo M, Joosten MH, Peck SC (2004) Activity profiling of papain-like cysteine proteases in plants. Plant Physiol **135:** 1170–1178

van Esse HP, Bolton MD, Stergiopoulos I, de Wit PJ, Thomma BP (2007) The chitin-binding *Cladosporium fulvum* effector protein Avr4 is a virulence factor. Mol Plant Microbe Interact **20:** 1092–1101

van Esse HP, Van't Klooster JW, Bolton MD, Yadeta KA, van Baarlen P, Boeren S, Vervoort J, de Wit PJ, Thomma BP (2008) The *Cladosporium fulvum* virulence protein Avr2 inhibits host proteases required for basal defense. Plant Cell **20:** 1948–1963

van Loon LC, Rep M, Pieterse CM (2006) Significance of inducible defense-related proteins in infected plants. Annu Rev Phytopathol **44:** 135–162

Vleeshouwers VGAA, van Dooijeweert W, Keizer LCP, Sijpkes L, Govers F, Colon LT (1999) A laboratory assay for Phytophthora infestans resistance in various Solanum species reflects the field situation. Eur J Plant Pathol **105:** 241–250

Wang Z, Gu C, Colby T, Shindo T, Balamurugan R, Waldmann H, Kaiser M, van der Hoorn RAL (2008) Beta-lactone probes identify a papain-like peptide ligase in *Arabidopsis thaliana*. Nat Chem Biol **4:** 557–563

Whisson SC, Boevink PC, Moleleki L, Avrova AO, Morales JG, Gilroy EM, Armstrong MR, Grouffaud S, van West P, Chapman S, et al (2007) A translocation signal for delivery of oomycete effector proteins into host plant cells. Nature **450:** 115–118

Yamada K, Matsushima R, Nishimura M, Hara-Nishimura I (2001) A slow maturation of a cysteine protease with a granulin domain in the vacuoles of senescing Arabidopsis leaves. Plant Physiol **127:** 1626–1634

Yang Z (2007) PAML 4: phylogenetic analysis by maximum likelihood. Mol Biol Evol **24:** 1586–1591

Yang Z, Wong WS, Nielsen R (2005) Bayes empirical Bayes inference of amino acid sites under positive selection. Mol Biol Evol **22:** 1107–1118

Zhang Z, Li J, Zhao XQ, Wang J, Wong GK, Yu J (2006) KaKs_Calculator: calculating Ka and Ks through model selection and model averaging. Genomics Proteomics Bioinformatics **4:** 259–263